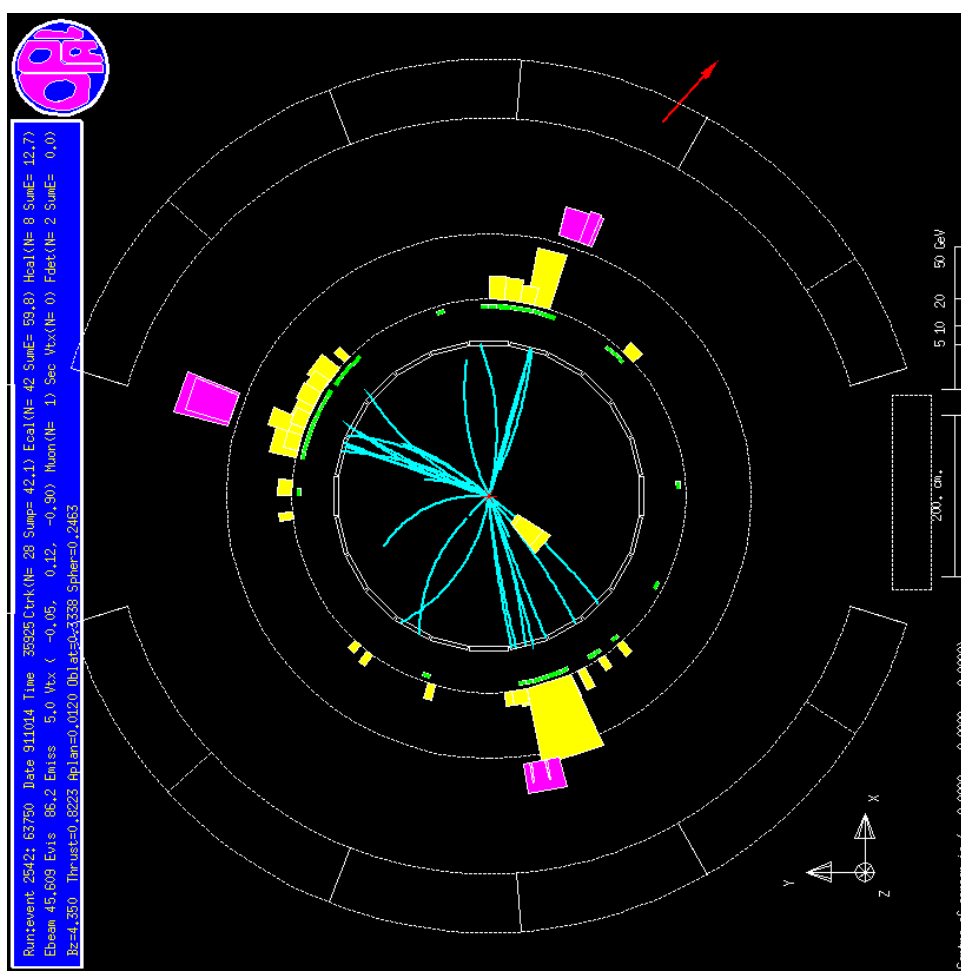


# Introduction to quantum chromodynamics (QCD)

Panos Christakoglou<sup>1,2</sup>



<sup>1</sup> P.Christakoglou@uu.nl - Utrecht University, Leonard S. Ornsteinlaboratorium Princetonplein 1, 3584CC Utrecht, The Netherlands

<sup>2</sup> Panos.Christakoglou@nikhef.nl - Nikhef, Science Park 105, 1098XG Amsterdam, The Netherlands



# Contents

<b>1</b>	<b>Introduction to Quantum Chromo Dynamics (QCD)</b>	<b>1</b>
1.1	A small recap from QED	1
1.2	The free Dirac equation	2
1.2.1	Global gauge invariance	3
1.2.2	Local gauge invariance	3
1.2.3	The interaction term	5
1.3	The field kinetic term	6
1.4	Some comments	8
1.5	QCD processes and Feynman diagrams	10
1.5.1	Feynman rules for QCD processes	11
1.5.2	QCD processes	13
1.6	Evidence of colour	13
1.7	The strong coupling strength	16
1.7.1	Numerical results of $\alpha_s$	18
1.8	Deep inelastic scattering	20
1.8.1	The parton model	20
1.8.2	Probing the quark and gluon distributions in protons	22



# Chapter 1

## Introduction to Quantum Chromo Dynamics (QCD)

The next pillar of the Standard Model that will be briefly presented is the one that describes the strong interactions. The gauge theory is called Quantum Chromo Dynamics or QCD and explains how the world of the smallest building blocks of ordinary matter, the quarks and the gluons, works. QCD shares a number of similarities with QED and thus we will profit from the prior experience that we gained from Chapter ?? to explore the fundamental properties of our theory. However, it is essential to point out that QCD, being by far more complicated than QED, has a number of fundamental differences compared to the theory that is based on U(1) transformations. Thus a large part of the current chapter will be devoted to highlighting these differences.

Once again, we will start by the Dirac Lagrangian that describes the dynamics of a free particle, this time a quark. We will then impose a more complicated transformation described by the SU(3) group, the underlying group of QCD. The requirement of local gauge invariance will automatically lead us to the term of the QCD Lagrangian that reflects the interactions between the free particle and the field. The kinetic term of this field will be derived again from the Proca Lagrangian. Requiring local gauge invariance also for this term, will reveal the nature of the QCD field: eight massless fields, the gluons.

We will then proceed by looking at a number of QCD processes with the help of the, known to us by now, Feynman diagrams. After a small recap of the similarities and the differences between QED and QCD we will focus on one of the main, fundamental differences between the two gauge theories: we will see how the strong coupling constant behaves depending on how “soft“ or “hard“ a process is (reflected by the momentum transfer). This discussion will naturally lead to the introduction of two of the main characteristics of QCD: confinement and asymptotic freedom.

We will conclude the chapter by briefly discussing about QCD processes known as deep inelastic scattering. Through this discussion we are going to see how one can probe the distribution functions of valence and sea quarks inside nucleons. Finally, we will talk about the remaining part inside nucleons: the gluon distribution functions.

### 1.1 A small recap from QED

Let us briefly summarise the steps we followed in QED to derive the overall Lagrangian density of the gauge theory:

- We started off with the Dirac Lagrangian that describes a free particle (e.g. a lepton) of the form:

$$\mathcal{L} = i\bar{\Psi}\gamma_{\mu}\partial^{\mu}\Psi - m\bar{\Psi}\Psi$$

- We then made a transformation of the form  $U = e^{ig\Lambda}$ , that transforms the eigenfunction as  $\Psi' = e^{ig\Lambda}\Psi$ , where  $g$  is a constant and  $\Lambda$  is a scalar. This is, as we saw, a U(1) transformation, a rotation with a phase  $g\Lambda$ .
- We then promoted the transformation from global to local by adding a dependence of  $\Lambda$  on space and/or time such that  $\Lambda = \Lambda(\mathbf{x}, t) = \Lambda(x^{\mu})$ .
- Applying this local transformation to the Lagrangian density, we saw that

$$\mathcal{L}' = i\bar{\Psi}\gamma_\mu\partial^\mu\Psi + i\bar{\Psi}\gamma_\mu\left(ig\partial^\mu\Lambda\right)\Psi - m\bar{\Psi}\Psi \neq \mathcal{L}$$

- The second term of the previous equation is responsible for breaking the invariance. Why is the invariance broken? Because of the dependence of the scalar  $\Lambda$  on space and time (note that now  $\Lambda = \Lambda(\mathbf{x}, t) = \Lambda(x^\mu)$ ), which leads to

$$\partial^\mu\Psi' = \partial^\mu\left(e^{ig\Lambda}\Psi\right) = e^{ig\Lambda}\partial^\mu\Psi + ig e^{ig\Lambda}\partial^\mu\left(\partial^\mu\Lambda\right)\Psi = e^{ig\Lambda}\left[\partial^\mu + ig\left(\partial^\mu\Lambda\right)\right]\Psi \neq e^{ig\Lambda}\partial^\mu\Psi$$

- How do we cure this? We tried to absorb the term that breaks the invariance,  $\partial^\mu + ig\left(\partial^\mu\Lambda\right)$ , by introducing a covariant derivative  $D^\mu = \partial^\mu + ig\left(\partial^\mu\Lambda\right)$  in the place of the partial derivative  $\partial^\mu$ .
- This automatically leads to the introduction of a new vector field  $A^\mu$ , such that  $D^\mu = \partial^\mu + igA^\mu$ .
- We then request local gauge invariance. Since this can't be achieved with the partial derivative, we use the newly introduced covariant derivative, such that after the U(1) transformation we demand that

$$D'_\mu\Psi' = e^{ig\Lambda}D_\mu\Psi$$

- It turned out that in order to have local gauge invariance the external vector field  $A^\mu$  should transform with a given rule, namely

$$A'_\mu = A_\mu - \partial_\mu\Lambda$$

- Adding then the covariant derivative  $D^\mu$  in the place of the partial derivative  $\partial^\mu$  in the free Dirac Lagrangian gives:

$$\mathcal{L} = i\bar{\Psi}\gamma_\mu D^\mu\Psi - m\bar{\Psi}\Psi = \bar{\Psi}\left(i\gamma_\mu\partial^\mu\Psi - m\right)\Psi - g\bar{\Psi}\gamma_\mu A^\mu\Psi$$

- The first term in the previous equation (i.e.  $\bar{\Psi}\left(i\gamma_\mu\partial^\mu\Psi - m\right)\Psi$ ) describes the free Dirac Lagrangian density for a lepton or a quark. The second term (i.e.  $g\bar{\Psi}\gamma_\mu A^\mu\Psi$ ) is the interaction term.
- To get the full Lagrangian density of the gauge theory we then added the Proca Lagrangian that describes the field itself:

$$\mathcal{L} = -\frac{1}{4}F_{\mu\nu}F^{\mu\nu} + \frac{1}{2}m^2 A_\mu A^\mu$$

- Applying the same U(1) transformation as before also for this term and requesting local gauge invariance leads to  $\mathcal{L}' = \mathcal{L} \Rightarrow m = 0$ . This implies that the gauge field is massless i.e. the photon.
- Finally, we also saw that the electromagnetic tensor  $F_{\mu\nu} = \partial_\mu A_\nu - \partial_\nu A_\mu$  can be derived by its gauge invariant form:  $[D_\mu, D_\nu] = igF_{\mu\nu}$ .

## 1.2 The free Dirac equation

For the case of QCD, we will start again with the Dirac Lagrangian that describes, this time, a free quark:

$$\mathcal{L} = i\bar{\Psi}\gamma_\mu\partial^\mu\Psi - m\bar{\Psi}\Psi \tag{1.2.1}$$

As in the case of QED, also here, we are going to act on it with a transformation. The underlying group that describes the relevant transformations in QCD is not as simple as U(1). These transformations are now described by  $3 \times 3$  matrices, described by the generators of the SU(3) group. The SU(3) transformation is now of the form

$$U = e^{ig\frac{\lambda}{2}\Lambda}, \quad (1.2.2)$$

where  $\Lambda$  are eight parameters associated with the eight gauge bosons of the theory i.e. the gluons. The matrices  $\lambda$  are all  $3 \times 3$  matrices also known as Gell-Mann matrices with the form:

$$\begin{aligned} \lambda_1 &= \begin{pmatrix} 0 & 1 & 0 \\ 1 & 0 & 0 \\ 0 & 0 & 0 \end{pmatrix}, \quad \lambda_2 = \begin{pmatrix} 0 & -i & 0 \\ i & 0 & 0 \\ 0 & 0 & 0 \end{pmatrix}, \quad \lambda_3 = \begin{pmatrix} 1 & 0 & 0 \\ 0 & -1 & 0 \\ 0 & 0 & 0 \end{pmatrix}, \quad \lambda_4 = \begin{pmatrix} 0 & 0 & 1 \\ 0 & 0 & 0 \\ 1 & 0 & 0 \end{pmatrix}, \\ \lambda_5 &= \begin{pmatrix} 0 & 0 & -i \\ 0 & 0 & 0 \\ i & 0 & 0 \end{pmatrix}, \quad \lambda_6 = \begin{pmatrix} 0 & 0 & 0 \\ 0 & 0 & 1 \\ 0 & 1 & 0 \end{pmatrix}, \quad \lambda_7 = \begin{pmatrix} 0 & 0 & 0 \\ 0 & 0 & -i \\ 0 & i & 0 \end{pmatrix}, \quad \lambda_8 = \frac{1}{\sqrt{3}} \begin{pmatrix} 1 & 0 & 0 \\ 0 & 1 & 0 \\ 0 & 0 & -2 \end{pmatrix} \end{aligned}$$

### 1.2.1 Global gauge invariance

Let us again first discuss the case where the transformation is global i.e. the parameters  $\Lambda$  are not a function of space and time but rather a constant. Is the Lagrangian density of Eq. 1.2.1 invariant under these types of transformations?

$$\begin{aligned} \mathcal{L}' &= i\bar{\Psi}' \gamma_\mu \partial^\mu \Psi' - m\bar{\Psi}' \Psi' \\ &= ie^{-ig\frac{\lambda}{2}\Lambda} \bar{\Psi} \gamma_\mu \partial^\mu (e^{ig\frac{\lambda}{2}\Lambda} \Psi) - me^{-ig\frac{\lambda}{2}\Lambda} \bar{\Psi} e^{ig\frac{\lambda}{2}\Lambda} \Psi \end{aligned}$$

Since  $\Lambda$  does not depend on space and time, it can be taken out from the partial derivative in the first term, such that:

$$\begin{aligned} \mathcal{L}' &= ie^{-ig\frac{\lambda}{2}\Lambda} e^{ig\frac{\lambda}{2}\Lambda} \bar{\Psi} \gamma_\mu \partial^\mu \Psi - me^{-ig\frac{\lambda}{2}\Lambda} e^{ig\frac{\lambda}{2}\Lambda} \bar{\Psi} \Psi \\ &= i\bar{\Psi} \gamma_\mu \partial^\mu \Psi - m\bar{\Psi} \Psi \Rightarrow \\ \mathcal{L}' &= \mathcal{L} \end{aligned}$$

We thus reach again the conclusion that our system, described by the Lagrangian density of Eq. 1.2.1, is invariant under global SU(3) transformations.

### 1.2.2 Local gauge invariance

We will now promote the transformation of Eq. 1.2.2 into a local one, by adding a dependence of  $\Lambda$  on space and/or time i.e.  $\Lambda = \Lambda(\mathbf{x}, t) = \Lambda(x^\mu)$ :

$$U = e^{ig\frac{\lambda}{2}\Lambda(x^\mu)}, \quad (1.2.3)$$

where  $g$  is still a constant and  $\Lambda$  this time is a scalar field. Let's look at how this transformation alters the Lagrangian density of Eq. 1.2.1 (note that I suppress in the lines below the dependence of  $\Lambda$  on  $x^\mu$ , however the reader should not misinterpret it as if the dependence is not there!!!):

$$\begin{aligned}\mathcal{L}' &= i\bar{\Psi}' \gamma_\mu \partial^\mu \Psi' - m\bar{\Psi}' \Psi' \\ &= ie^{-ig\Lambda} \bar{\Psi} \gamma_\mu \partial^\mu \left( e^{ig\Lambda} \Psi \right) - me^{-ig\Lambda} \bar{\Psi} e^{ig\Lambda} \Psi\end{aligned}$$

Note that  $\Lambda$  is not a constant but a scalar field i.e. a field whose value depends on space and time. That means that we can not just take it out from the partial derivative of the first term, but instead the derivative has to act on  $\Lambda(x^\mu)$ :

$$\begin{aligned}\mathcal{L}' &= ie^{-ig\frac{\lambda}{2}\Lambda} \bar{\Psi} \gamma_\mu \left( \partial^\mu e^{ig\frac{\lambda}{2}\Lambda} \right) \Psi + ie^{-ig\frac{\lambda}{2}\Lambda} \bar{\Psi} \gamma_\mu e^{ig\frac{\lambda}{2}\Lambda} \left( \partial^\mu \Psi \right) - me^{-ig\frac{\lambda}{2}\Lambda} e^{ig\frac{\lambda}{2}\Lambda} \bar{\Psi} \Psi \\ &= ie^{-ig\frac{\lambda}{2}\Lambda} \bar{\Psi} \gamma_\mu \left( ig\frac{\lambda}{2} \right) e^{ig\frac{\lambda}{2}\Lambda} \left( \partial^\mu \Lambda \right) \Psi + i\bar{\Psi} \gamma_\mu \partial^\mu \Psi - m\bar{\Psi} \Psi \\ &= -g\frac{\lambda}{2} \bar{\Psi} \gamma_\mu \left( \partial^\mu \Lambda \right) \Psi + i\bar{\Psi} \gamma_\mu \partial^\mu \Psi - m\bar{\Psi} \Psi \\ &= -g\frac{\lambda}{2} \bar{\Psi} \gamma_\mu \left( \partial^\mu \Lambda \right) \Psi + \mathcal{L} \neq \mathcal{L}\end{aligned}$$

It is thus clear that the Lagrangian does not remain invariant under this local gauge transformation. The first term in the equation above is responsible for this, with the underlying reason being that the exponent that describes the transformation can not be taken out from the partial derivative:  $\partial^\mu$  has to act on  $e^{ig\Lambda(x^\mu)}$  since now  $\Lambda$  is not a constant but a scalar field that depends on  $x^\mu$ .

Let's look again a bit closer at the responsible term:

$$\partial^\mu \Psi' = \partial^\mu \left( e^{ig\frac{\lambda}{2}\Lambda} \Psi \right) = e^{ig\frac{\lambda}{2}\Lambda} \partial^\mu \Psi + ig\frac{\lambda}{2} \left( \partial^\mu \Lambda \right) \Psi = e^{ig\frac{\lambda}{2}\Lambda} \left[ \partial^\mu + ig\frac{\lambda}{2} \left( \partial^\mu \Lambda \right) \right] \Psi \neq e^{ig\frac{\lambda}{2}\Lambda} \partial^\mu \Psi$$

The idea is the same as in the case of QED, it is just the term that needs to be absorbed is a bit more complicated since it involves the  $\lambda$ -matrices. So how about trying to absorb the term  $\left[ \partial^\mu + ig\frac{\lambda}{2} \left( \partial^\mu \Lambda \right) \right]$  which is responsible for breaking the invariance into a new quantity that will be built for the exact purpose of restoring the desired invariance of the Lagrangian density?

For this reason we introduce the covariant derivative  $D^{\mu\mu}$  constructed in a way to have the desired property:

$$D^{\mu'} \Psi' = e^{ig\frac{\lambda}{2}\Lambda} D^\mu \Psi$$

The term responsible for breaking the invariance of the Lagrangian density,  $\left[ \partial^\mu + ig\frac{\lambda}{2} \left( \partial^\mu \Lambda \right) \right]$ , once again motivates the form of the covariant derivative:

$$D^\mu = \partial^\mu + ig\frac{\lambda}{2} A^\mu, \quad (1.2.4)$$

where  $A^\mu$  are eight external vector fields. So from now on, we need to replace in the Lagrangian density the term  $\partial^\mu \Psi$  with  $D^\mu \Psi$ . The latter provides us with the feature of  $D^{\mu'} \Psi' = e^{ig\frac{\lambda}{2}\Lambda} D^\mu \Psi$  we need. Here comes another complication: due to the fact that  $A^\mu$  are eight gauge fields, we need to introduce another index to keep track of this:

$$D^\mu \equiv \partial^\mu + ig\frac{\lambda^\alpha}{2} A^{\mu\alpha}, \quad (1.2.5)$$

We now investigate how the external fields should transform to ensure that local gauge invariance is preserved. For this we need  $D^{\mu'} \Psi' = e^{ig\frac{\lambda^\alpha}{2}\Lambda^\alpha} D^\mu \Psi$ . Let us look at the different terms one by one:



- Let us first look at the term  $D^{\mu'}\Psi'$ :

$$\begin{aligned} D^{\mu'}\Psi' &= \left(\partial^\mu + ig\frac{\lambda^\alpha}{2}A^{\mu\alpha}\right)\left(e^{ig\frac{\lambda^\alpha}{2}A^{\mu\alpha}}\Psi\right) = \\ &\partial^\mu\left(e^{ig\frac{\lambda^\alpha}{2}A^{\mu\alpha}}\Psi\right) + ig\frac{\lambda^\alpha}{2}A^{\mu\alpha'}e^{ig\frac{\lambda^\alpha}{2}A^{\mu\alpha}}\Psi = \\ &e^{ig\frac{\lambda^\alpha}{2}A^{\mu\alpha}}\left(\partial^\mu\Psi\right) + ig\frac{\lambda^\alpha}{2}e^{ig\frac{\lambda^\alpha}{2}A^{\mu\alpha}}\left(\partial^\mu A^\alpha\right)\Psi + ig\frac{\lambda^\alpha}{2}A^{\mu\alpha'}e^{ig\frac{\lambda^\alpha}{2}A^{\mu\alpha}}\Psi \end{aligned}$$

- Next, we look at the term  $e^{ig\frac{\lambda^\alpha}{2}A^\alpha}D^\mu\Psi$ :

$$\begin{aligned} e^{ig\frac{\lambda^\alpha}{2}A^\alpha}D^\mu\Psi &= e^{ig\frac{\lambda^\alpha}{2}A^\alpha}\left(\partial^\mu + ig\frac{\lambda^\alpha}{2}A^{\mu\alpha}\right)\Psi = \\ &e^{ig\frac{\lambda^\alpha}{2}A^\alpha}\left(\partial^\mu\Psi\right) + ig e^{ig\frac{\lambda^\alpha}{2}A^\alpha}\frac{\lambda^\alpha}{2}A^{\mu\alpha}\Psi \end{aligned}$$

Comparing those two terms, it turns out that the external fields should transform in a rather complicated manner, given by:

$$e^{ig\frac{\lambda^\alpha}{2}A^\alpha}\lambda^\alpha A^{\mu\alpha} = \lambda^\alpha A^{\mu\alpha'}e^{ig\frac{\lambda^\alpha}{2}A^\alpha} + \lambda^\alpha e^{ig\frac{\lambda^\alpha}{2}A^\alpha}\left(\partial^\mu A^\alpha\right) \quad (1.2.6)$$

This complicated transformation that the external fields need to obey stems from the fact that, contrary to the U(1) case, in SU(3) the matrices  $\lambda^\alpha$  and the gauge fields  $A^{\mu\alpha}$  do not commute. In the vocabulary of group theory, this means that SU(3) is not Abelian.

### 1.2.3 The interaction term

With the previous requirement we have ensured that local gauge invariance is preserved and we can safely write down the QCD Lagrangian density of the free quark field:

$$\begin{aligned} \mathcal{L}_{\text{QCD}} &= i\bar{\Psi}\gamma_\mu D^\mu\Psi - m\bar{\Psi}\Psi = \\ &i\bar{\Psi}\gamma_\mu\left(\partial^\mu + ig\frac{\lambda^\alpha}{2}A^{\mu\alpha}\right)\Psi - m\bar{\Psi}\Psi = \\ &i\bar{\Psi}\gamma_\mu\partial^\mu\Psi - m\bar{\Psi}\Psi - g\bar{\Psi}\gamma_\mu\frac{\lambda^\alpha}{2}A^{\mu\alpha}\Psi \rightarrow \\ \mathcal{L}_{\text{QCD}}^{\text{partial}} &= \bar{\Psi}(i\gamma_\mu\partial^\mu - m)\Psi - g\bar{\Psi}\gamma_\mu\frac{\lambda^\alpha}{2}A^{\mu\alpha}\Psi \quad (1.2.7) \end{aligned}$$

The first term of Eq. 1.2.7 is the standard Lagrangian density of the free particle i.e. the quark. The second term that was introduced, involves both the spinors  $\bar{\Psi}$  and  $\Psi$  but also the external vector fields  $A^{\mu\alpha}$ . This is the interaction term! This term introduced by the requirement of local gauge invariance, reflects the interactions between the particles (i.e. quarks in this case) with the external field.

### 1.3 The field kinetic term

So far our theory consists of the term that describes the free particle with mass  $m$  (i.e. the free quark) and the term that describes the interaction of the particle with the vector fields (i.e. the interaction term). To complete our theory we need to include also the term that describes the field itself. This term comes once again from the Proca Lagrangian described in Section ??:

$$\mathcal{L} = -\frac{1}{4}F_{\mu\nu}F^{\mu\nu} + \frac{1}{2}M^2A_\mu A^\mu, \quad (1.3.1)$$

where  $F_{\mu\nu}$  is the field tensor of the theory. Let us note again that in this equation,  $M$  is the mass of the vector fields, whereas in Eq. 1.2.1  $m$  corresponds to the mass of the particle that feels the field i.e. the quark in this case.

We now apply the transformation of Eq. 1.2.3 in Eq. ??:

$$\mathcal{L}' = -\frac{1}{4}F'_{\mu\nu}F'^{\mu\nu} + \frac{1}{2}m^2A'_\mu A'^\mu$$

At this point, I will not repeat the same tedious mathematical steps that we did in Section ?. In addition to the fact that the procedure is practically the same, the vector fields in QCD have a highly not trivial transformation they need to obey (see Eq. 1.2.6). This fact adds some additional number of lines of algebraic actions that one needs to follow. Nevertheless, if one completes all the steps we will once again reach the conclusion that in order for local gauge invariance to be preserved also for the field term, then the fields need to be massless (i.e.  $M = 0$ ). So we have eight (since our theory is described by SU(3) that has eight generators) massless fields: the eight physical gluons!!!

After setting the mass of the vector fields to zero, the term that remains is the one that has the tensor ‘‘squared’’: i.e.  $-\frac{1}{4}F_{\mu\nu}F^{\mu\nu}$ . In the case of QED, where the underlying group was the one of U(1), the tensor was simply given by  $F_{\mu\nu} = \partial_\mu A_\nu - \partial_\nu A_\mu$ . But this term in QCD, described by SU(3), is not anymore gauge invariant! However we know very well how to construct such a term in a way that local gauge invariant is not at question: we will use the equation

$$[D_\mu, D_\nu] = igF_{\mu\nu} \rightarrow F_{\mu\nu} = \frac{-i}{g}[D_\mu, D_\nu]$$

The advantage is obvious: the field tensor is constructed from the commutator of the covariant derivatives. Remember that the covariant derivatives were introduced in a way to absorb the terms that were breaking local gauge invariance. Therefore, preserving local gauge invariance is in that way guaranteed. In what follows, we will derive the form of the field tensor. For that, it is easier (i.e. it will make the place where different partial derivatives act more clear) if we let the previous equation act on a spinor field, such that  $F_{\mu\nu}\Psi = \frac{-i}{g}[D_\mu, D_\nu]\Psi$ .

$$\begin{aligned} \frac{-i}{g}[D_\mu, D_\nu]\Psi &= -\frac{i}{g}\left(\partial_\mu + ig\frac{\lambda^\alpha}{2}A_\mu^\alpha\right)\left(\partial_\nu + ig\frac{\lambda^\beta}{2}A_\nu^\beta\right)\Psi + \frac{i}{g}\left(\partial_\nu + ig\frac{\lambda^\beta}{2}A_\nu^\beta\right)\left(\partial_\mu + ig\frac{\lambda^\alpha}{2}A_\mu^\alpha\right)\Psi = \\ &= -\frac{i}{g}\partial_\mu(\partial_\nu\Psi) + \frac{\lambda^\alpha}{2}A_\mu^\alpha(\partial_\nu\Psi) + \frac{\lambda^\beta}{2}A_\nu^\beta(\partial_\mu\Psi) + ig\frac{\lambda^\alpha}{2}A_\mu^\alpha\frac{\lambda^\beta}{2}A_\nu^\beta\Psi - \frac{i}{g}\partial_\mu\left(ig\frac{\lambda^\beta}{2}A_\nu^\beta\right)\Psi \\ &+ \frac{i}{g}\partial_\nu(\partial_\mu\Psi) - \frac{\lambda^\beta}{2}A_\nu^\beta(\partial_\mu\Psi) - \frac{\lambda^\alpha}{2}A_\mu^\alpha(\partial_\nu\Psi) - ig\frac{\lambda^\beta}{2}A_\nu^\beta\frac{\lambda^\alpha}{2}A_\mu^\alpha\Psi + \frac{i}{g}\partial_\nu\left(ig\frac{\lambda^\alpha}{2}A_\mu^\alpha\right)\Psi = \\ &= \frac{ig}{4}\left(\lambda^\alpha A_\mu^\alpha\lambda^\beta A_\nu^\beta - \lambda^\beta A_\nu^\beta\lambda^\alpha A_\mu^\alpha\right) + \frac{1}{2}\partial_\mu\left(\lambda^\beta A_\nu^\beta\right)\Psi - \frac{1}{2}\partial_\nu\left(\lambda^\alpha A_\mu^\alpha\right)\Psi = \\ &= \frac{ig}{4}\left[\lambda^\alpha A_\mu^\alpha, \lambda^\beta A_\nu^\beta\right] + \frac{1}{2}\left[\lambda^\beta(\partial_\mu A_\nu^\beta) - \lambda^\alpha(\partial_\nu A_\mu^\alpha)\right] = \end{aligned}$$

$$\frac{ig}{4} [\lambda^\alpha A_\mu^\alpha, \lambda^\beta A_\nu^\beta] + \frac{1}{2} \lambda^\alpha (\partial_\mu A_\nu^\alpha - \partial_\nu A_\mu^\alpha)$$

In the last two lines, the last terms imply using the summation rule for indices with indices  $\alpha$  and  $\beta$ . But the  $\lambda$ -matrices can be considered the same i.e. both their indices run from 1 to 8 at the same time, and thus can factorise. As for the commutator, the first term of the previous equation, we have to use again the summation rule for indices. We can then pull out of the commutator the vector fields  $A_\mu$  and  $A_\nu$  such that:

$$[\lambda^\alpha A_\mu^\alpha, \lambda^\beta A_\nu^\beta] = [\lambda^\alpha, \lambda^\beta] A_\mu^\alpha A_\nu^\beta$$

The commutator is not zero due to the Gell-Mann matrices! The generators of SU(3) respect the following Algebra:

$$[\lambda^\alpha, \lambda^\beta] = if^{\alpha\beta\gamma} \lambda^\gamma, \quad (1.3.2)$$

where the variables  $f^{\alpha\beta\gamma}$  are real numbers, called the structure constants of SU(3).

Let's now identify the final form of the field tensor (note that we will interchange the indices  $\alpha$ ,  $\beta$  and  $\gamma$  compared to what we followed before to make the final expression more convenient in writing; there is no essential change with this action):

$$\begin{aligned} F_{\mu\nu} &= \frac{ig}{4} [\lambda^\beta, \lambda^\gamma] A_\mu^\beta A_\nu^\gamma + \frac{1}{2} \lambda^\alpha (\partial_\mu A_\nu^\alpha - \partial_\nu A_\mu^\alpha) = \frac{ig}{4} f^{\alpha\beta\gamma} \lambda^\alpha A_\mu^\beta A_\nu^\gamma + \frac{1}{2} \lambda^\alpha (\partial_\mu A_\nu^\alpha - \partial_\nu A_\mu^\alpha) \Rightarrow \\ F_{\mu\nu} &= \frac{1}{2} \lambda^\alpha (\partial_\mu A_\nu^\alpha - \partial_\nu A_\mu^\alpha) - \frac{g}{4} f^{\alpha\beta\gamma} \lambda^\alpha A_\mu^\beta A_\nu^\gamma \end{aligned} \quad (1.3.3)$$

Once again, we can pull out the  $\lambda^\alpha$  matrices so that the field tensor can take the following form:

$$F_{\mu\nu} = \lambda^\alpha F_{\mu\nu}^\alpha, \quad (1.3.4)$$

where  $F_{\mu\nu}^\alpha = \frac{1}{2} (\partial_\mu A_\nu^\alpha - \partial_\nu A_\mu^\alpha) - \frac{g}{4} f^{\alpha\beta\gamma} A_\mu^\beta A_\nu^\gamma$ .

We are not done since the final QCD Lagrangian density had the field tensor ‘‘squared’’. It is enough to see what kind of complications this brings by simply looking at the ‘‘square’’ of the  $F_{\mu\nu}^\alpha$  part:

$$\begin{aligned} F_{\mu\nu}^\alpha F^{\mu\nu\alpha} &= \left[ \frac{1}{2} (\partial_\mu A_\nu^\alpha - \partial_\nu A_\mu^\alpha) - \frac{g}{4} f^{\alpha\beta\gamma} A_\mu^\beta A_\nu^\gamma \right] \left[ \frac{1}{2} (\partial^\mu A^{\nu\alpha} - \partial^\nu A^{\mu\alpha}) - \frac{g}{4} f^{\alpha\delta\epsilon} A^{\mu\delta} A^{\nu\epsilon} \right] = \\ &= \frac{1}{4} (\partial_\mu A_\nu^\alpha - \partial_\nu A_\mu^\alpha) (\partial^\mu A^{\nu\alpha} - \partial^\nu A^{\mu\alpha}) \\ &\quad - \frac{g}{8} f^{\alpha\beta\gamma} A_\mu^\beta A_\nu^\gamma (\partial_\mu A_\nu^\alpha - \partial_\nu A_\mu^\alpha) \\ &\quad - \frac{g}{8} f^{\alpha\delta\epsilon} (\partial_\mu A_\nu^\alpha - \partial_\nu A_\mu^\alpha) A^{\mu\delta} A^{\nu\epsilon} \\ &\quad - \frac{g^2}{16} f^{\alpha\beta\gamma} f^{\alpha\delta\epsilon} A_\mu^\beta A_\nu^\gamma A^{\mu\delta} A^{\nu\epsilon} \end{aligned}$$

Let us try to understand what each term brings:

- $\frac{1}{4} (\partial_\mu A_\nu^\alpha - \partial_\nu A_\mu^\alpha) (\partial^\mu A^{\nu\alpha} - \partial^\nu A^{\mu\alpha})$ : This first term of the previous equation is the standard term for the field we encountered also in QED (modulo the factor 1/4 which is not relevant).

- $\frac{g}{8} f^{\alpha\beta\gamma} A_{\mu}^{\beta} A_{\nu}^{\gamma} (\partial_{\mu} A_{\nu}^{\alpha} - \partial_{\nu} A_{\mu}^{\alpha})$ : This term contains “interactions“ between three vector fields e.g.  $A_{\mu}^{\beta} A_{\nu}^{\gamma} \partial_{\mu} A_{\nu}^{\alpha}$ . These terms reveal one of the main differences between QED and QCD which have to do with vertices involving three gluons.
- $\frac{g}{8} f^{\alpha\delta\epsilon} (\partial_{\mu} A_{\nu}^{\alpha} - \partial_{\nu} A_{\mu}^{\alpha}) A^{\mu\delta} A^{\nu\epsilon}$ : Similarly to the term before, also this term contains “interactions“ between three vector fields e.g.  $\partial_{\mu} A_{\nu}^{\alpha} A^{\mu\delta} A^{\nu\epsilon}$ . These terms describe again vertices that involve three gluons.
- $\frac{g^2}{16} f^{\alpha\beta\gamma} f^{\alpha\delta\epsilon} A_{\mu}^{\beta} A_{\nu}^{\gamma} A^{\mu\delta} A^{\nu\epsilon}$ : This term clearly involves “interactions“ between four vector fields and describe vertices that involve four gluons.

These last elements, which are characteristic of QCD are shown in fig. 1.1.

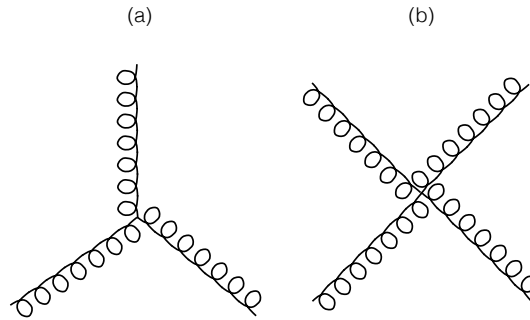


Fig. 1.1: One of the main characteristic QCD feature: the self coupling of the gauge bosons of the theory originating from its non-Abelian nature i.e. the three and four gluon vertices.

## 1.4 Some comments

At this stage it is once again essential to take a break and reflect on a few things. Let me guide you through with the following comments:

- As in the case of QED, also in QCD, we acted on the Dirac Lagrangian of the free particle with a transformation. The underlying group that describes the relevant transformations in QCD is not as simple as  $U(1)$ . These transformations are now described by  $3 \times 3$  matrices, described by the generators of the  $SU(3)$  group.

But how do we act on the eigenfunction  $\Psi$  with such a complicated transformation that obeys the properties and rules of the  $SU(3)$  group? The answer is that we have to make  $\Psi$  a bit more complicated as well: the eigenfunction needs to have this time three additional elements:

$$\Psi = (\Psi_R, \Psi_B, \Psi_G) \quad (1.4.1)$$

where each component of the new array corresponds to the new quantum number associated with the strong interaction i.e. the colour:  $\Psi_R$  for red,  $\Psi_B$  for blue and  $\Psi_G$  for green.

Remember though that that  $\Psi$  in the Dirac equations was a 4–component vector representing two particles with spin  $\pm 1/2$  and two antiparticles with similar as before spin orientation of  $\pm 1/2$ . That means that this new 3–component spinor comes on top of the existing four components! These three components are different colour charges of each element of the 4–component Dirac spinor!!! An extra dimension on the existing spinor, but this time explicitly for quarks.

- A few words about the “charge“ and its nature in QED and in QCD. In QED the word “charge“ was associated to the electric charge. It had two possible values  $\pm 1$ : a positive and a negative charge always an integer multiple of the charge of the electron.

In QCD on the other had, the word “charge“ is associated to the colour charge. We have seen that we have three charges: red, blue and green. Note that as in the case of QED, also in QCD, each of these charges have two possible values: R and  $\bar{R}$ , B and  $\bar{B}$ , G and  $\bar{G}$ .

Overall, it looks as if QCD contains three times the QED fundamental structure. In the language of group theory, people say that the maximum commuting subgroup of  $SU(3)$  is  $U(1) \times U(1) \times U(1)$ .

- Each quark has a colour chosen between the three available i.e. R, B and G. Each antiquark has an anticolour chosen between the three available i.e.  $\bar{R}$ ,  $\bar{B}$  and  $\bar{G}$ . Gluons have one colour and one anticolour.

The basis vectors in colour space are

$$C_1 = |R\rangle = \begin{pmatrix} 1 \\ 0 \\ 0 \end{pmatrix}$$

$$C_2 = |B\rangle = \begin{pmatrix} 0 \\ 1 \\ 0 \end{pmatrix}$$

$$C_3 = |G\rangle = \begin{pmatrix} 0 \\ 0 \\ 1 \end{pmatrix}$$

Their Hermitian conjugates are:

$$C_1^\dagger = \langle R| = (1 \ 0 \ 0)$$

$$C_2^\dagger = \langle B| = (0 \ 1 \ 0)$$

$$C_3^\dagger = \langle G| = (0 \ 0 \ 1)$$

- There are eight physical gauge bosons in QCD, as expected by the fact that the underlying group that describes the strong interactions is  $SU(3)$  that has eight generators. Each gluon contains one colour and one anticolour. The physical states are written as follows:

$$\begin{aligned} |1\rangle &= \frac{1}{\sqrt{2}} \begin{pmatrix} R\bar{B} + B\bar{R} \end{pmatrix} & |2\rangle &= \frac{-i}{\sqrt{2}} \begin{pmatrix} R\bar{B} - B\bar{R} \end{pmatrix} \\ |3\rangle &= \frac{1}{\sqrt{2}} \begin{pmatrix} R\bar{R} - B\bar{B} \end{pmatrix} & |4\rangle &= \frac{1}{\sqrt{2}} \begin{pmatrix} R\bar{G} + G\bar{R} \end{pmatrix} \\ |5\rangle &= \frac{-i}{\sqrt{2}} \begin{pmatrix} R\bar{G} - G\bar{R} \end{pmatrix} & |6\rangle &= \frac{1}{\sqrt{2}} \begin{pmatrix} B\bar{G} + G\bar{B} \end{pmatrix} \\ |7\rangle &= \frac{-i}{\sqrt{2}} \begin{pmatrix} B\bar{G} - G\bar{B} \end{pmatrix} & |8\rangle &= \frac{1}{\sqrt{6}} \begin{pmatrix} R\bar{R} + B\bar{B} - 2G\bar{G} \end{pmatrix} \end{aligned}$$

- The  $SU(3)$  transformation that is applied is, as we have seen, of the form  $U = e^{ig\frac{\lambda}{2}A}$ . The matrices  $\lambda$  are all  $3 \times 3$  matrices also known as Gell-Mann matrices with the form:

$$\begin{array}{cccc}
 \underbrace{\begin{pmatrix} 0 & 1 & 0 \\ 1 & 0 & 0 \\ 0 & 0 & 0 \end{pmatrix}}_{\lambda_1} & \underbrace{\begin{pmatrix} 0 & -i & 0 \\ i & 0 & 0 \\ 0 & 0 & 0 \end{pmatrix}}_{\lambda_2} & \underbrace{\begin{pmatrix} 1 & 0 & 0 \\ 0 & -1 & 0 \\ 0 & 0 & 0 \end{pmatrix}}_{\lambda_3} & \underbrace{\begin{pmatrix} 0 & 0 & 1 \\ 0 & 0 & 0 \\ 1 & 0 & 0 \end{pmatrix}}_{\lambda_4} \\
 \underbrace{\begin{pmatrix} 0 & 0 & -i \\ 0 & 0 & 0 \\ i & 0 & 0 \end{pmatrix}}_{\lambda_5} & \underbrace{\begin{pmatrix} 0 & 0 & 0 \\ 0 & 0 & 1 \\ 0 & 1 & 0 \end{pmatrix}}_{\lambda_6} & \underbrace{\begin{pmatrix} 0 & 0 & 0 \\ 0 & 0 & -i \\ 0 & i & 0 \end{pmatrix}}_{\lambda_7} & \frac{1}{\sqrt{3}} \underbrace{\begin{pmatrix} 1 & 0 & 0 \\ 0 & 1 & 0 \\ 0 & 0 & -2 \end{pmatrix}}_{\lambda_8}
 \end{array}$$

- There are, as we have seen, eight physical gluon states. These states are in fact reflected in the Gell-Mann matrices if one writes the general form of the matrix as

$$\begin{pmatrix} \overline{R\overline{R}} & \overline{R\overline{B}} & \overline{R\overline{G}} \\ \overline{B\overline{R}} & \overline{B\overline{B}} & \overline{B\overline{G}} \\ \overline{G\overline{R}} & \overline{G\overline{B}} & \overline{G\overline{G}} \end{pmatrix}$$

The Gell-Mann matrices have the colours of each gluon state embedded in them!

- Why is the underline group of QCD the one of  $SU(3)$  and not the one of  $U(3)$ ? After all, the generators of  $U(3)$  are also  $3 \times 3$  matrices. The reason is that in that case there would be a ninth gluon whose form would be

$$|9\rangle = \frac{1}{\sqrt{3}} (\overline{R\overline{R}} + \overline{B\overline{B}} + \overline{G\overline{G}})$$

Note that this is a colour singlet state. Remember that all naturally observed particles are in a colour singlet state and thus the ninth gluon would qualify as one i.e. we would be able to see gluons flying free in nature!!! Since this is not observed, then this means that this gluon state does not exist, it is not physical!

- We have seen in Section 1.3 how the fact that  $SU(3)$  is a non-Abelian group leads to additional terms in the QCD Lagrangian density revealed by the introduction of the field kinetic term. These three and four gluon vertices highlight the self-coupling nature of the gauge bosons of QCD.

## 1.5 QCD processes and Feynman diagrams

In this section we are going to review some basic QCD processes. These processes involve interactions between particles that have obviously the ability to feel the strong force i.e. the quarks and gluons. But the quarks and the gluons are not seen free in nature. As a result the processes we are about to briefly review happen but are not directly seen in experiments. They are only observed indirectly via e.g. the production of spray of hadrons within a very narrow cone usually referred to as jet production. Nevertheless, understanding and measuring such processes to various measurements is very critical: it is obviously critical to measure cross-sections of various QCD processes if you started with this aim but that's not the end of the story. In accelerators that offer collisions between particles formed by partonic<sup>1</sup> constituents and in particular at very high energies these QCD processes are the dominant contribution in searches of particle physics experiments. A characteristic example of such case is the Large Hadron Collider where protons are collided against protons with the main goal of the experimental physics program of three out of the four major experiments (i.e. ATLAS, CMS and LHCb) being the exploration of the standard model within its electroweak sector. But more on this in Chapters ?? and ??.

At this point let me remind you that in Chapter ??, we have seen what is the way one can calculate the cross-section of a process. We have to calculate the so-called matrix element,  $M_{if}$ , that describes the transition from the initial to the final state. The calculation of the matrix element is facilitated by the so-called Feynman diagrams and the corresponding rules. Below, we summarise the basic Feynman rules for QCD for completeness and we then take a look at some of the basic

<sup>1</sup> This is the first time the term "parton" appears in these lecture notes. Get used to it since it will be used from now on a number of times. When writing parton one refers to the quarks and the gluons of a composite particle.

QCD processes. Note again that the calculation of the matrix element of a process using the Feynman rules is beyond the scope of this course, this is why there is no such attempt here.

### 1.5.1 Feynman rules for QCD processes

Let's now review how these general rules described before change in the case of a strong interaction.

Let's now review how these general rules described before change in the case of an electromagnetic or weak interaction.

- **Labeling:** We label every external line with the ingoing and outgoing momenta  $\mathbf{P}_1, \dots, \mathbf{P}_n$ , adding also an arrow indicating whether a particle is approaching or moving away from the vertex. If the diagram includes antiparticles, we still label them as particles but with the reverse direction of the arrow. We then label the 4-momenta for all internal lines  $\mathbf{q}_1, \dots, \mathbf{q}_j$  and we give an arbitrary direction to the relevant arrow.
- **External lines:** Each external line contribute the following factors:

$$\text{Incoming quark} \rightarrow u^s \cdot c$$

$$\text{Outgoing quark} \rightarrow \bar{u}^s \cdot c^\dagger$$

$$\text{Incoming anti-quark} \rightarrow \bar{v}^s \cdot c^\dagger$$

$$\text{Outgoing anti-quark} \rightarrow v \cdot c$$

$$\text{Incoming gluon} \rightarrow \varepsilon_\mu \cdot a^\alpha$$

$$\text{Outgoing gluon} \rightarrow \varepsilon_\mu^* \cdot a^{\alpha*}$$

where  $u$  and  $v$  are the relevant Dirac spinors. In the previous  $c$  are the matrices that represent the colour:

$$\begin{pmatrix} 1 \\ 0 \\ 0 \end{pmatrix} \text{ for R, } \begin{pmatrix} 0 \\ 1 \\ 0 \end{pmatrix} \text{ for G, } \begin{pmatrix} 0 \\ 0 \\ 1 \end{pmatrix} \text{ for B}$$

and  $a$  are the 8-element column matrices, one for each gluon state (i.e.  $\alpha$  goes from 1 to 8):

$$|1\rangle \equiv \begin{pmatrix} 1 \\ 0 \\ 0 \\ 0 \\ 0 \\ 0 \\ 0 \\ 0 \end{pmatrix}, |2\rangle \equiv \begin{pmatrix} 0 \\ 1 \\ 0 \\ 0 \\ 0 \\ 0 \\ 0 \\ 0 \end{pmatrix}, |3\rangle \equiv \begin{pmatrix} 0 \\ 0 \\ 1 \\ 0 \\ 0 \\ 0 \\ 0 \\ 0 \end{pmatrix}, |4\rangle \equiv \begin{pmatrix} 0 \\ 0 \\ 0 \\ 1 \\ 0 \\ 0 \\ 0 \\ 0 \end{pmatrix}, |5\rangle \equiv \begin{pmatrix} 0 \\ 0 \\ 0 \\ 0 \\ 1 \\ 0 \\ 0 \\ 0 \end{pmatrix}, |6\rangle \equiv \begin{pmatrix} 0 \\ 0 \\ 0 \\ 0 \\ 0 \\ 1 \\ 0 \\ 0 \end{pmatrix}, |7\rangle \equiv \begin{pmatrix} 0 \\ 0 \\ 0 \\ 0 \\ 0 \\ 0 \\ 1 \\ 0 \end{pmatrix}, |8\rangle \equiv \begin{pmatrix} 0 \\ 0 \\ 0 \\ 0 \\ 0 \\ 0 \\ 0 \\ 1 \end{pmatrix}$$

- **Vertices:** For each vertex we note down in the diagram the coupling constant factor  $\approx g_s$ . This factor is connected to the coupling constant via the equation

$$g_s = \sqrt{4\pi\alpha_s}$$

For a quark-gluon vertex (see fig. 1.2) the factor is of the form:

$$\frac{-ig_s}{2} \lambda^\alpha \gamma^\mu$$

where the parameters  $\lambda^\alpha$  are the Gell-Man  $\lambda$ -matrices of SU(3).

For a 3-gluon vertex (see fig. 1.2) the factor is of the form:

$$-g_s f^{\alpha\beta\gamma} \left[ g_{\mu\nu}(\mathbf{k}_1 - \mathbf{k}_2)_\rho + g_{\nu\rho}(\mathbf{k}_2 - \mathbf{k}_3)_\mu + g_{\rho\mu}(\mathbf{k}_3 - \mathbf{k}_1)_\nu \right]$$

where the factors  $f^{\alpha\beta\gamma}$  are the structure constants of SU(3) and  $\mathbf{k}_i$  are the 4-momenta of each internal line (with  $i = 1, 2, 3$ ).

Finally, for a 4-gluon vertex (see fig. 1.2) the factor is of the form:

$$-ig_s^2 \left[ f^{\alpha\beta\eta} f^{\gamma\delta\eta} (g_{\mu\sigma} g_{\nu\rho} - g_{\mu\rho} g_{\nu\sigma}) + f^{\alpha\delta\eta} f^{\beta\gamma\eta} (g_{\mu\nu} g_{\sigma\rho} - g_{\mu\sigma} g_{\nu\rho}) + f^{\alpha\gamma\eta} f^{\delta\beta\eta} (g_{\mu\rho} g_{\nu\sigma} - g_{\mu\nu} g_{\sigma\rho}) \right]$$

- **Propagators:** For each internal line, we give a factor of

$$q - \bar{q} : \frac{i(\not{q} + m)}{\mathbf{q}^2 - m^2}$$

$$\text{gluon} : -ig_{\mu\nu} \delta^{\alpha\beta}$$

where  $\not{q} \equiv \gamma_\nu q^\nu$ .

- **$\delta$ -functions and integration:** The remaining steps are identical as in the general rules described before.

Figure 1.2 presents the lines for the basic particles and anti-particles but also the propagators for the strong interactions.

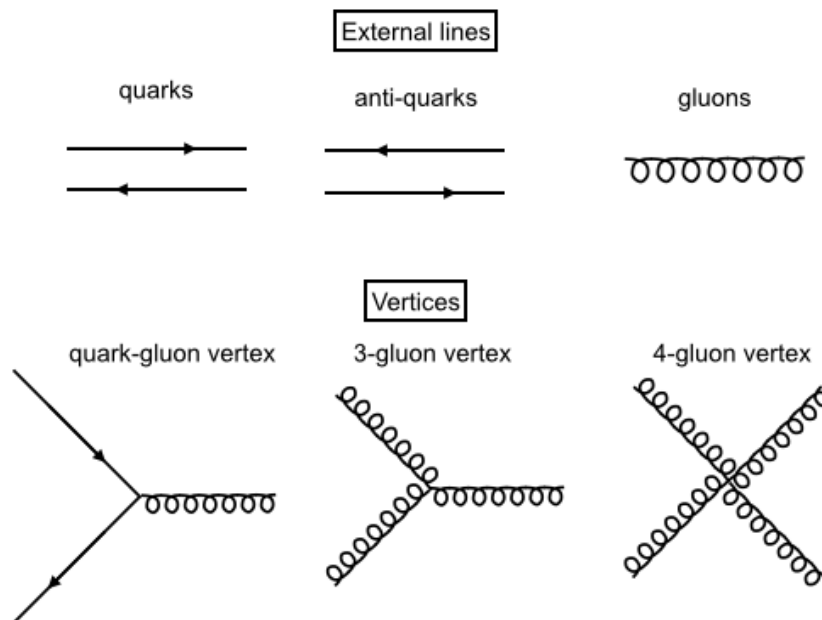


Fig. 1.2: The most characteristic lines for the Feynman diagrams in strong interactions.



### 1.5.2 QCD processes

There are three main categories of basic QCD processes that we will review. In all cases what is important to note is that colour needs to be conserved on every vertex. The processes consist of:

- interactions between quarks where only one colour is involved (e.g. fig. 1.3–a),
- interactions between quarks where two colours are involved, but there is no colour exchange at the vertex (e.g. fig. 1.3–b)
- interactions between quarks where two colours are involved with colour exchange at the vertex (e.g. fig. 1.3–c)

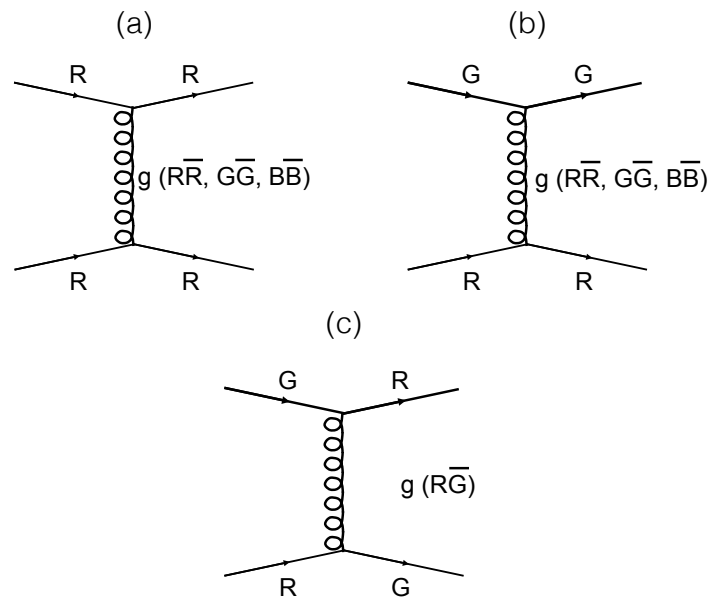


Fig. 1.3: Basic QCD processes with an illustration of how colour is conserved at the vertices.

In fig. 1.3–a the interaction involves two red quarks. This interaction is facilitated with the exchange of any of the colourless gluon states among the eight we have introduced i.e.  $|3\rangle$  or  $|8\rangle$ .

In fig. 1.3–b the interaction takes place between a red quark and a green quark. It can be seen that colour is not altered between the incoming and the outgoing partons i.e. left and right relative to each vertex. As a result the transition is again facilitated with the exchange of any of the colourless gluon states among the eight we have introduced i.e.  $|3\rangle$  or  $|8\rangle$ .

Finally, in fig. 1.3–c the interaction takes place between a red quark and a green quark similarly as in the previous case. However, this time the process involves a change of colour at each vertex. If one focuses on the bottom vertex, then the gluon needs to have such a colour combination to compensate for the incoming red and the outgoing green colours. As a result the gluon needs to have the  $R\bar{G}$  combination. Similarly in the upper vertex, the gluon needs to carry such a colour combination to compensate for the incoming green and the outgoing red colours. That means that the needed combination is the  $\bar{G}R$ . This means that the transition is facilitated with the exchange of any of the  $|4\rangle$  or  $|5\rangle$  gluon states among the eight we have introduced.

## 1.6 Evidence of colour

So far we have discussed about colour as a new quantum number that characterises quarks and gluons. We have not discussed how the existence of colour was established. To do this, we need to go back to a QED process we should be

by now familiar with i.e. the electron-positron scattering described by the interaction  $e^- + e^+ \rightarrow \mu^- + \mu^+$  and by the diagram 1.4.

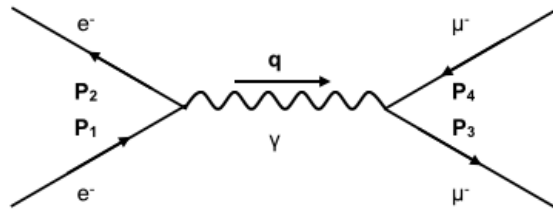


Fig. 1.4: The diagram describing the electron-positron scattering into a pair of muons  $e^- + e^+ \rightarrow \mu^- + \mu^+$ .

Similarly to this figure, one can as well create a pair of quarks i.e. more precise a  $q - \bar{q}$  pair that for a brief moment fly apart until they are separated by a distance of the size of the hadron ( $\approx 10^{-15}$  m). The relevant diagram for this process is given in fig. 1.5. Beyond this distance it is energetically favourable to form new  $q - \bar{q}$  pairs that eventually lead to the creation of hadrons. It turns out though that the initial  $q - \bar{q}$  pair leaves a footprint in the final state hadron production since these hadrons usually emerge as two back-to-back sprays, known as jets. In some cases it happens that a gluon emerges with a substantial fraction of the initial energy. This gluon then fragments, creating a third jet, a topology known as a three-jet event. Examples of a two- and three-jet events are shown in the left and right plot of fig. 1.6, respectively.

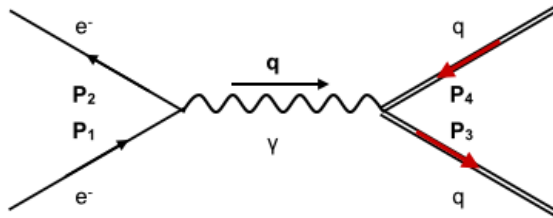


Fig. 1.5: The diagram describing the electron-positron scattering into a pair of quarks  $e^- + e^+ \rightarrow q + \bar{q}$ .

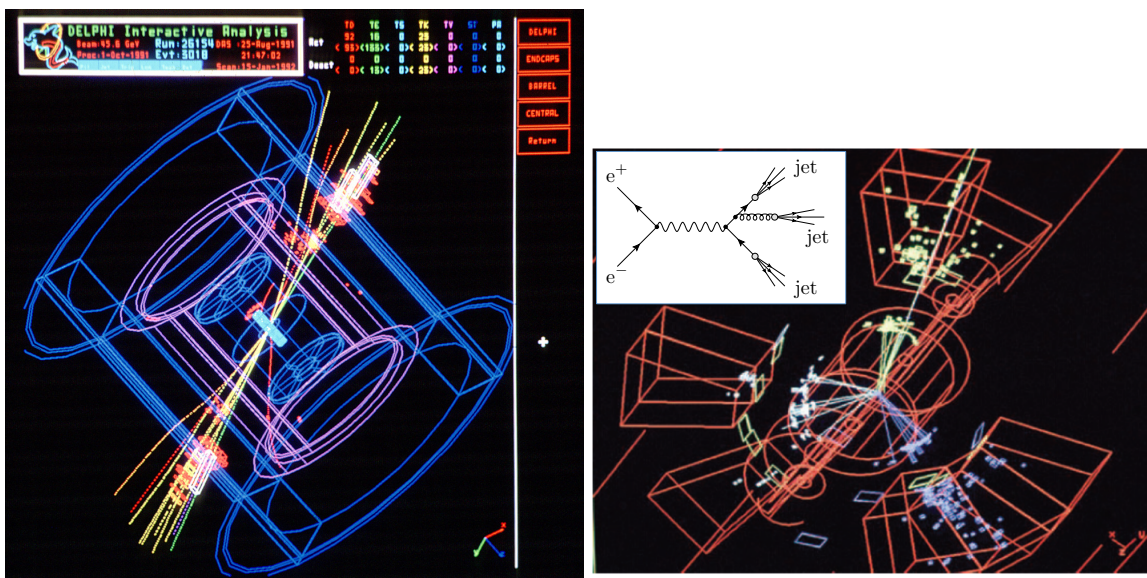


Fig. 1.6: A typical two- and three-jet topology in the left and right plot, respectively.

At the Large Hadron Collider (LHC), where the energy compared to the previous colliders has increased significantly i.e. by orders of magnitude, we are able to detect event topologies that involve more than three jets. That implies that more than one gluon carries enough energy, fragment and produce additional jets. An example of a five jet event topology from the ATLAS experiment is given in fig. 1.7

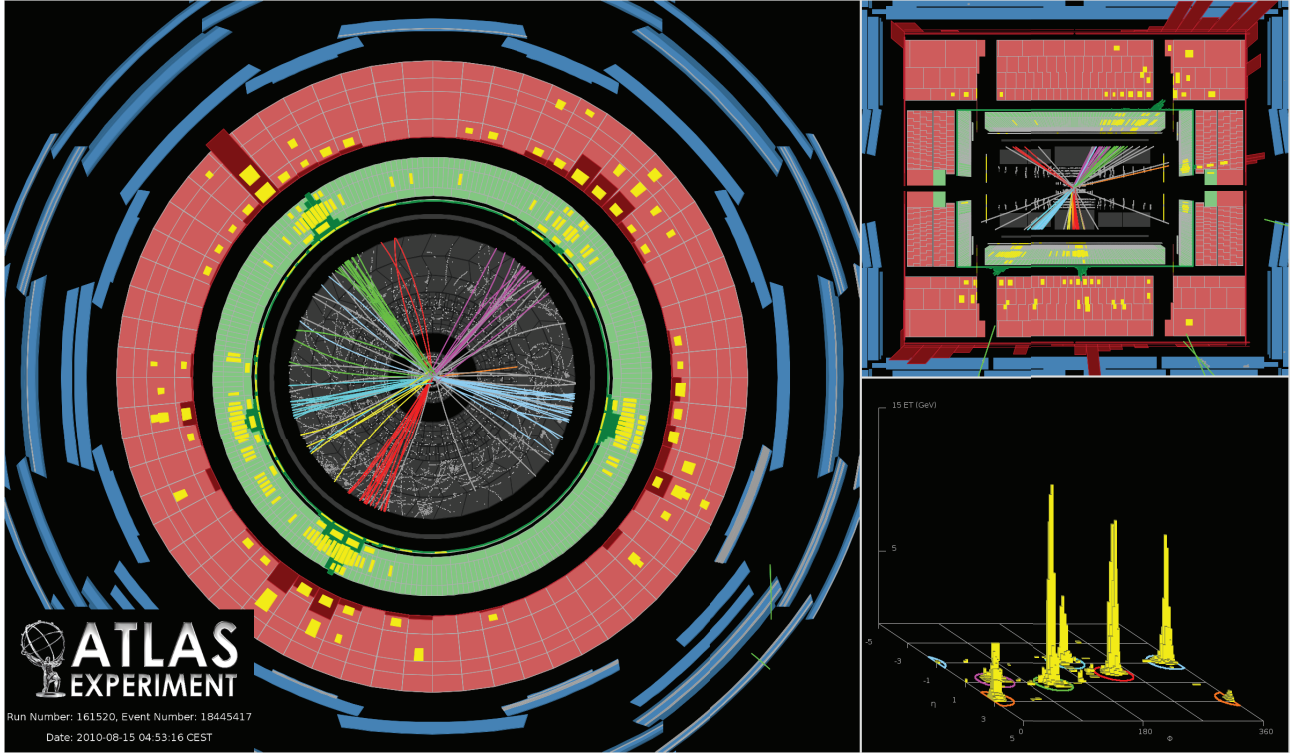


Fig. 1.7: A typical five-jet topology as recorded by the ATLAS experiment at the LHC.

In terms of the incident energy  $E$  of the electron (positron) and the scattering angle  $\theta$  between the electron and the quark, the squared average matrix element is given by

$$\langle |M_{if}|^2 \rangle = Q^2 g_e^4 \left[ 1 + \left(\frac{m}{E}\right)^2 + \left(\frac{M}{E}\right)^2 + \left(1 - \left(\frac{m}{E}\right)^2\right) \cdot \left(1 - \left(\frac{M}{E}\right)^2\right) \cos^2(\theta) \right]$$

It is obvious that there is a threshold for this interaction to occur:  $E \geq M$ , below which the process is kinematically forbidden. The final integrated cross-section for the case where  $E > M \gg m$  is

$$\sigma = \frac{\pi}{3} \left[ \frac{Q\alpha}{E} \right]^2 \quad (1.6.1)$$

As the energy increases, new quarks are allowed to be created e.g. at about 1.5 GeV the charm quark.

Through the comparison between the cross-sections for the processes  $e^- + e^+ \rightarrow q + \bar{q}$  and  $e^- + e^+ \rightarrow \mu^- + \mu^+$ , one can probe the number of colours via the ratio

$$R = \frac{\sigma(e^- + e^+ \rightarrow \text{hadrons})}{\sigma(e^- + e^+ \rightarrow \mu^- + \mu^+)} \quad (1.6.2)$$

Since the numerator includes all possible  $q - \bar{q}$  pairs, Eq. 1.6.1 gives:

$$R(E) = 3 \sum Q_i^2,$$

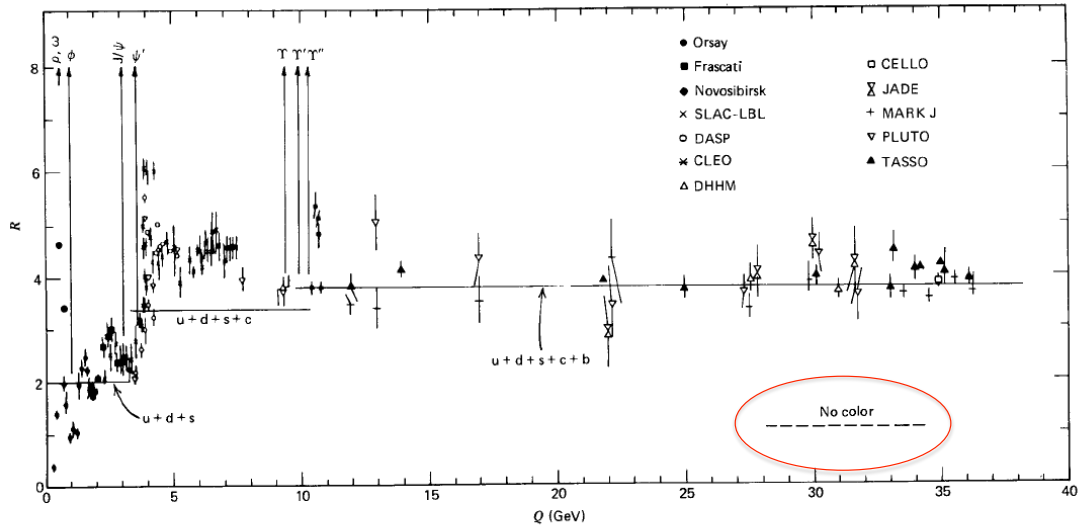


**Fig. 11.3** Ratio  $R$  of (11.6) as a function of the total  $e^+e^-$  center-of-mass energy. (The sharp peaks correspond to the production of narrow  $1^-$  resonances just below or near the flavor thresholds.)

Fig. 1.8: The energy evolution of  $R$  as measured in experiments.

where the sum is over all quark flavours with threshold below  $E$  and the factor 3 in front of the summation reflects the fact that there are three colours for each flavour. For  $u$ ,  $d$ , and  $s$  quarks one expects to have:

$$R = 3 \left[ \left( \frac{2}{3} \right)^2 + \left( \frac{-1}{3} \right)^2 + \left( \frac{-1}{3} \right)^2 \right] = 2$$

Above the threshold for the  $c$ -quark:  $R = 2 + 3(2/3)^2 = 10/3$ , above the threshold for the  $b$ -quark  $R = 10/3 + 3(-1/3)^2 = 11/3$ . One expects a staircase evolution, depending on the threshold and certainly something that reflects the existence of three colours. Figure 1.8 present the energy evolution of  $R$  as measured in experiments.

## 1.7 The strong coupling strength

We have seen in Chapter ?? how an electron is surrounded by a cloud of virtual photons and  $e^+e^-$  pairs continuously pop in and out of existence. This charge screening gives rise to the notion of an effective charge  $e(r)$  that becomes smaller with larger distance. One says that the  $\beta$ -function is positive in QED:

$$\beta(r) \equiv - \frac{de(r)}{d \ln r}$$

Likewise, the QCD vacuum consists of virtual  $q\bar{q}$  pairs, and if this would be all, the charge screening mechanism would be the same as in QED, with a positive  $\beta$ -function. However, due to the gluon self-coupling, the vacuum will also

be filled with virtual gluon pairs as is indicated in fig. 1.9. Because the gluon cloud carries colour charge, it turns out that the effective charge becomes larger with larger distance. Hence, the *beta*-function is negative. This effect is called antiscreening.<sup>2</sup> It turns out that the negative contribution wins over the positive contribution, so that the QCD beta function is negative, and the effective strong coupling becomes small at short distances.

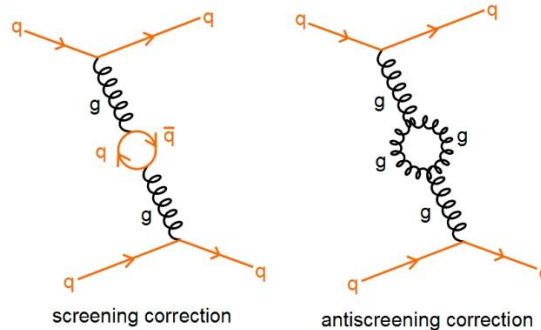


Fig. 1.9: The photon vacuum polarisation (left) generates a charge screening effect, making  $\alpha$  smaller at larger distances.

Charge screening in QED and antiscreening QCD leads to the concept of a running coupling. In QED we have seen that the coupling becomes large at (very) short distance but its effect is small. In QCD, the antiscreening effect causes the strong coupling to become small at short distance (large momentum transfer). This causes the quarks inside hadrons to behave more or less as free particles, when probed at large enough energies. This property of the strong interaction is called asymptotic freedom. Asymptotic freedom allows us to use perturbation theory, and by this arrive at quantitative predictions for hard scattering cross sections in hadronic interactions. On the other hand, at increasing distance the coupling becomes so strong that it is impossible to isolate a quark from a hadron (it becomes cheaper to create a  $q$  quark-antiquark pair). This mechanism is called confinement. Confinement is verified in Lattice QCD calculations but, since it is non-perturbative, not mathematically proven from first principles.

The discovery of asymptotic freedom (1973) was a major breakthrough for QCD as the theory of the strong interaction, and was awarded the Nobel prize in 2004 to Gross, Politzer and Wilczek.<sup>3</sup> To get a more quantitative insight into asymptotic freedom, we will now first discuss the higher order corrections and the running coupling in QED.

Let's now turn explicitly to the strong coupling constant  $\alpha_s$ . Note that  $\alpha_s$  is large, compared to the electromagnetic coupling constant  $\alpha = 1/137$ : strong interactions are indeed strong. The running is also strong, compared to a few percent effect at large  $Q^2$  in QED. The running of  $\alpha_s$  is beautifully confirmed by experiment. For  $Q^2 \sim 1$ ,  $\alpha_s \sim 1$  and perturbative QCD breaks down. Usually  $Q^2 \sim 5-10 \text{ GeV}^2$  is considered to be reasonable lower bound for perturbation theory to apply.

$$\alpha_s(Q^2) = \frac{\alpha_s(\mu^2)}{1 + \beta_0 \alpha_s(\mu^2) \ln(Q^2/\mu^2)} \quad \text{with} \quad \beta_0 = \frac{11N_c - 2n_f}{12\pi}$$

Because  $\beta_0 > 0$  we find that  $\alpha_s \rightarrow 0$  for  $Q^2 \rightarrow \infty$ . This vanishing coupling is called asymptotic freedom and is responsible for the fact that quarks behave like free particles at short distances (large momentum transfers) as is observed in deep inelastic scattering experiments. The expression for the running coupling constant can be simplified when we define the QCD scale parameter  $\Lambda$  as follows:

$$\frac{1}{\alpha_s(Q^2)} = \frac{1}{\alpha_s(\mu^2)} + \beta_0 \ln\left(\frac{Q^2}{\mu^2}\right) \equiv \beta_0 \ln\left(\frac{Q^2}{\Lambda^2}\right)$$

The parameter  $\Lambda$  is thus equal to the scale where the first term on the right-hand side vanishes, that is, the scale where  $\alpha_s(\mu^2)$  becomes infinite. Now we may write

<sup>2</sup> Antiscreening follows from the calculation of vacuum polarisation in QCD, which is non-trivial and beyond the scope of these lectures; unfortunately it is not so easy to intuitively understand the antiscreening effect.

<sup>3</sup> The Nobel lecture of Frank Wilczek can be downloaded from <http://www.nobelprize.org> and makes highly recommended reading, both as an exposé of the basic ideas, and as a record of the hard struggle.

$$\alpha_s(Q^2) = \frac{1}{\beta_0 \ln(Q^2/\Lambda^2)}$$

Experimentally, the value of  $\Lambda$  is found to be about 300 MeV, but the scale parameter is nowadays out of fashion because it cannot be defined unambiguously beyond 1-loop order. Instead, it is now common practise to not quote a value for  $\Lambda$ , but a value for  $\alpha_s$  at the mass of the Z. This is unambiguous at all orders. At  $Q^2$  values close to  $\Lambda$ , the coupling constant becomes large and perturbative QCD breaks down.

### 1.7.1 Numerical results of $\alpha_s$

Beside the quark masses, the only free parameter in the QCD Lagrangian is the strong coupling constant  $\alpha_s$ . The coupling constant in itself is not a physical observable, but rather a quantity defined in the context of perturbation theory, which enters predictions for experimentally measurable observables, such as  $R$  we have encountered in Section ??.

Many experimental observables are used to determine  $\alpha_s$ . The simplest observables in QCD are those that do not involve initial-state hadrons and that are fully inclusive with respect to details of the final state. One example is the total cross section for  $e^+e^- \rightarrow$  hadrons at center-of-mass energy  $Q$ , for which one can write:

$$R = \frac{\sigma(e^- + e^+ \rightarrow \text{hadrons})}{\sigma(e^- + e^+ \rightarrow \mu^- + \mu^+)} = R_{EW}(Q) [1 + \delta_{QCD}(Q)] \quad (1.7.1)$$

where  $R_{EW}(Q)$  is the purely electroweak prediction for the ratio and  $\delta_{QCD}(Q)$  is the correction due to QCD effects. To keep the discussion simple, we can restrict our attention to energies  $Q \ll M_Z$ , where the process is dominated by photon exchange ( $R_{EW} = 3 \sum_q e_q^2$ , neglecting finite-quark-mass corrections, where the  $e_q$  are the electric charges of the quarks):

$$\delta_{QCD}(Q) = \sum_{n=1}^{\infty} c_n \left[ \frac{\alpha_s(Q^2)}{\pi} \right]^n + \mathcal{O}\left(\frac{\Lambda^4}{Q^4}\right)$$

Considerations in such determinations include:

- The observable's sensitivity to  $\alpha_s$  as compared to the experimental precision. For example, for the  $e^+e^-$  cross section to hadrons, QCD effects are only a small correction, since the perturbative series starts at order  $\alpha_s^0$ ; 3-jet production or event shapes in  $e^+e^-$  annihilations are directly sensitive to  $\alpha_s$  since they start at order  $\alpha_s$ ; the hadronic decay width of heavy quarkonia,  $\Gamma(\Upsilon \rightarrow \text{hadrons})$ , is very sensitive to  $\alpha_s$  since its leading order term is  $\approx \alpha_s^3$ .
- The accuracy of the perturbative prediction, or equivalently of the relation between  $\alpha_s$  and the value of the observable. The minimal requirement is generally considered to be an NLO prediction. Some observables are predicted to NNLO (many inclusive observables, 3-jet rates and event shapes in  $e^+e^-$  collisions) or even N<sup>3</sup>LO ( $e^+e^-$  hadronic cross section and the branching fraction to hadrons). In certain cases, fixed-order predictions are supplemented with resummation.
- The size of uncontrolled non-perturbative effects. Sufficiently inclusive quantities, like the  $e^+e^-$  cross section to hadrons, have small non-perturbative uncertainties  $\approx \Lambda/Q^4$ .

#### 1.7.1.1 Results from deep inelastic scattering (DIS)

New measurements of  $\alpha_s$  from inclusive jet cross sections in  $\gamma\gamma$  interactions at HERA are available from the ZEUS collaboration. Jet cross sections and values of  $\alpha_s$  are presented as a function of the jet transverse energy,  $E_T^{jet}$ , for jets with  $E_T^{jet} > 17$  GeV. The resulting values of  $\alpha_s(E_T^{jet})$ , based on NLO QCD calculations, are in good agreement with the running of  $\alpha_s$ , as expected by QCD, and average to:

$$\alpha_s(M_{Z^0}) = 0.1224 \pm 0.0001 \text{ (stat.)}$$

$$\begin{array}{l} +0.0022 \\ -0.0019 \end{array} \text{ (exp.)}$$

$$\begin{array}{l} +0.0054 \\ -0.0042 \end{array} \text{ (theo.)}, \quad (1.7.2)$$

if evolved to the energy scale of  $M_{Z^0}$  using the QCD  $\beta$  function in two-loop approximation. Averaging all measurements of  $\alpha_s$  from jet production at HERA results in:

$$\alpha_s(M_{Z^0}) = 0.120 \pm 0.002 \text{ (exp.)}$$

$$\pm 0.004 \text{ (theo.)}, \quad (1.7.3)$$

A new global analysis using all available precision data of deep inelastic and related hard scattering processes includes recent measurements of structure functions from HERA and of the inclusive jet cross sections at the Tevatron. After analysis of experimental and theoretical uncertainties the authors obtain

$$\alpha_s(M_{Z^0}) = 0.1165 \pm 0.002 \text{ (exp.)}$$

$$\pm 0.003 \text{ (theo.)}, \quad (1.7.4)$$

in NLO QCD. Using NNLO QCD calculations wherever available, the same fit gives:

$$\alpha_s(M_{Z^0}) = 0.1153 \pm 0.002 \text{ (exp.)}$$

$$\pm 0.003 \text{ (theo.)}. \quad (1.7.5)$$

The latter result, however, does not relate to complete NNLO since predictions of jet production cross sections and parts of the DIS structure functions are only available in NLO so far.

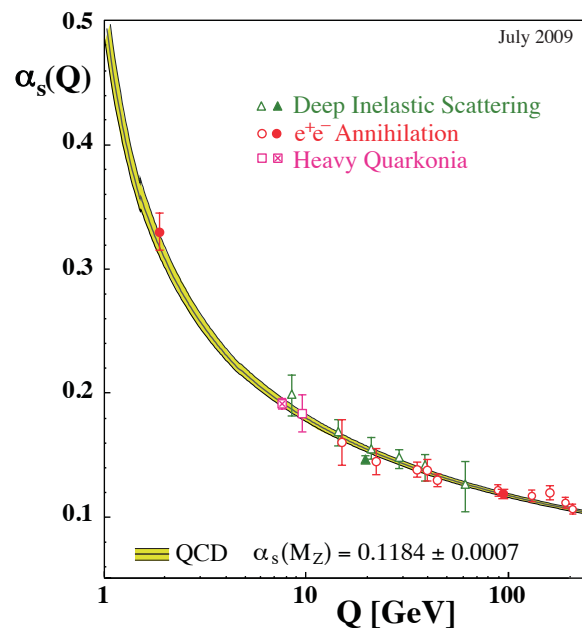


Fig. 1.10: The  $Q$  dependence of the strong coupling constant  $\alpha_s$ .

The wealth of available results provides a rather precise and stable world average value of  $\alpha_s(M_Z)$ , as well as a clear signature and proof of the energy dependence of  $\alpha_s$ , in full agreement with the QCD prediction of asymptotic freedom.

This is demonstrated in fig. 1.10, where results of  $\alpha_s(Q)$  obtained at discrete energy scales  $Q$ , now also including those based just on NLO QCD, are summarized. Thanks to the results from the Tevatron and from the LHC, the energy scales at which  $\alpha_s$  is determined now extend to several hundred GeV up to 1 TeV.

## 1.8 Deep inelastic scattering

One way to probe the internal structure of matter is to bombard it with high energy particles, and then see what happens. For instance, in the Rutherford experiment (1911), alpha particles (helium nuclei) were deflected on a thin gold foil. Rutherford found that the deflections followed his famous inverse  $\sin^4(\theta/2)$  law, and concluded that the alpha particles were scattered from electrically charged point-like nuclei inside the gold atoms. Experiments using probes of higher energy later revealed that the point-like scattering distributions were damped by form factors which are essentially the Fourier transform of a charge distribution. This clearly showed that nuclei are not point-like and indeed, after the discovery of the neutron by Chadwick (1932), it became clear that nuclei are bound states of protons and neutrons. Also the protons and neutrons were found not to be point-like and a real breakthrough came with a series of deep inelastic scattering experiments in the 1960's at SLAC, where electron beams were scattered on proton targets at energies of about 20 GeV, large enough to reveal the proton's internal structure. The SLAC experiments showed that the electrons were scattering off quasi-free point-like constituents inside the proton which were soon identified with quarks. This was the first time that quarks were shown to be dynamical entities, instead of bookkeeping devices to classify the hadrons (Gell-Mann's eightfold way). The Nobel prize was awarded in 1990 for this spectacular discovery.

The pioneering SLAC experiments were followed by a series of other fixed-target experiments<sup>4</sup> with larger energies at CERN (Geneva) and at Fermilab (Chicago), using electrons, muons, neutrino's and anti-neutrinos as probes. The largest centre-of-mass energies were reached at the HERA collider in Hamburg (1992–2007) with counter rotating beams of 27 GeV electrons and 800 GeV protons. Deep inelastic scattering (DIS) data are very important since they provide detailed information on the momentum distributions of the partons (quarks and gluons) inside the proton. Parton distributions are crucial ingredients in theoretical predictions of scattering cross-sections at hadron colliders like the Tevatron (Fermilab, proton-antiproton at 2 TeV) or the LHC (CERN, proton-proton at 5–14 TeV). The reason for this is simple: the colliding (anti)protons have a fixed centre-of-mass energy but not the colliding partons, since their momenta are distributed inside the (anti)proton. Clearly one has to fold-in this momentum spread to compare theoretical predictions with the data. Apart from providing parton distributions, DIS is also an important testing ground for perturbative QCD, as we will see.

### 1.8.1 The parton model

When a highly energetic virtual photon interacts with the proton, it probes its constituents i.e. the quarks and the gluons. However since the gluons do not interact with the photon, we can safely say that we mainly probe the quarks. Now, there are more than one type of such particles inside the proton. Each such quark, can carry a different fraction of the proton's momentum and energy. This is schematically depicted in fig. 1.11.

We now introduce the parton distribution function  $f_i(x)$  which gives the probability that the struck parton carries a fraction  $x$  of the proton's momentum  $P$ . All the fractions have to add up to unity such that:

$$\sum_i \int x f_i(x) dx = 1,$$

where the index  $i$  includes also the patrons that do not interact with the virtual photon. Note that in a dynamical picture, inside the proton there are also gluons from the QCD splitting  $q \rightarrow qg$  and quark-antiquark pairs from the splitting  $g \rightarrow q\bar{q}$ . What is true is that there is a net excess of three quarks that carry the quantum numbers of the proton. A schematic picture of the QCD proton structure is given in fig. 1.12. The  $uud$  that carry the quantum numbers of the proton enter the diagram

<sup>4</sup> In a fixed-target experiment, beam particles interact with a stationary target in the laboratory, and the debris is recorded in a downstream detector. In a collider experiment, on the other hand, counter-rotating beams collide in the centre of a detector, which is built around the interaction region.



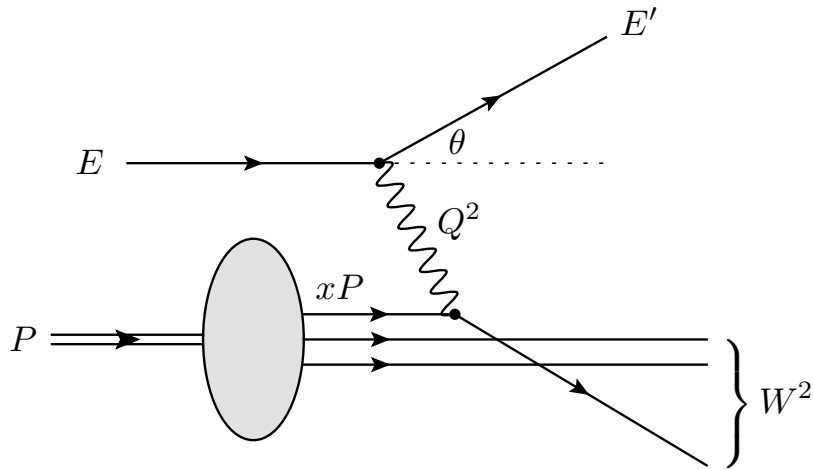


Fig. 1.11: The interaction of a highly energetic virtual photon with the quark of the initial proton that carries a fraction  $x$  of its momentum.

on the left, and they are called the **valence quarks**. This corresponds to a low-resolution 3-quark picture of the proton that only accounts for its quantum numbers. At the right of the diagram we see a high-resolution picture (at large  $Q^2$ ) of the proton where the valence quarks are dressed with gluons and a **sea** of  $q\bar{q}$  pairs. Note that the valence quarks can zig-zag through the diagram but will never disappear so that the proton quantum numbers are the same in both the low- and high-resolution pictures.

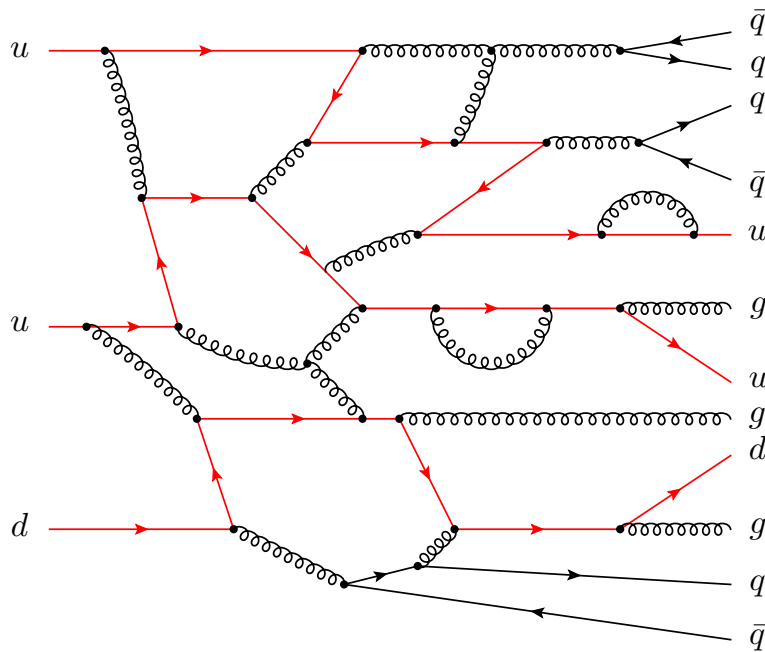


Fig. 1.12: The dynamical picture of the proton, with the valence and sea quarks and the gluons.

### 1.8.2 Probing the quark and gluon distributions in protons

As indicated before, the proton has a more dynamical picture than the static one where only the valence quarks, that carry the quantum numbers, are prominent. There are not only gluons but also what is usually referred to as sea quarks. We will focus on the three lightest quark flavours i.e.  $u, d, s$  since the remaining heavy flavour quarks (i.e.  $c, b, t$ ) are subject to threshold effects for their production in the sea. Under these considerations, the  $F_2$  structure function, defined as the charge weighted sum of the parton momentum densities  $xf_i(x)$ , can be written as:

$$\frac{1}{x}F_2^p(x) = \left(\frac{2}{3}\right)^2 [u^p(x) + \bar{u}^p(x)] + \left(\frac{1}{3}\right)^2 [d^p(x) + \bar{d}^p(x)] + \left(\frac{1}{3}\right)^2 [s^p(x) + \bar{s}^p(x)],$$

where e.g.  $u(x)$  and  $\bar{u}(x)$  are the probability distributions of  $u$  and  $\bar{u}$  quarks within the proton. This structure function has obviously six unknown quantities. To overcome this one relies on the fact that the proton and the neutron are members of an isospin doublet and thus their quark content is related. The inelastic neutron structure functions can be constrained by scattering of electrons off a deuterium target:

$$\frac{1}{x}F_2^n(x) = \left(\frac{2}{3}\right)^2 [u^n(x) + \bar{u}^n(x)] + \left(\frac{1}{3}\right)^2 [d^n(x) + \bar{d}^n(x)] + \left(\frac{1}{3}\right)^2 [s^n(x) + \bar{s}^n(x)],$$

The quark contents between the proton and the neutron are the same if one reverses  $u$  for  $d$  (and vice-versa). This means that:

$$u^p(x) = d^n(x) \equiv u(x)$$

$$d^p(x) = u^n(x) \equiv d(x)$$

$$s^p(x) = s^n(x) \equiv s(x)$$

Another constrain for the currently unknown quantities comes from the fact that the quantum numbers of the proton are carried by the valence quarks. In addition, if we consider the dynamical picture of the proton, schematically introduced in fig. 1.12, one can assume that the sea quarks which are radiated by the valence quarks occur to first order at the same rate and have similar momentum distributions (please note that we still consider the three lightest flavours). It is convenient to define the valence and the sea quark distributions as:

$$\begin{aligned} u_v &= u - \bar{u}, & d_v &= d - \bar{d}, & s_v &= s - \bar{s} = 0, & \dots \\ u_s &= 2\bar{u}, & d_s &= 2\bar{d}, & s_s &= 2\bar{s}, & \dots \end{aligned}$$

so that  $u + \bar{u} = u_v + u_s$ , etc.

Summing over all contributing partons, we should recover the quantum number of the proton and thus we have the following counting rules:

$$\int_0^1 u_v(x) dx = 2 \quad \text{and} \quad \int_0^1 d_v(x) dx = 1$$

As a result the proton and neutron structure functions can be written as:

$$\frac{1}{x}F_2^p = \frac{1}{9} [4u_v + d_v] + \frac{4}{3}S$$

$$\frac{1}{x}F_2^n = \frac{1}{9} [u_v + 4d_v] + \frac{4}{3}S,$$

where  $S(x)$  is the sea quark distribution ( $u_s(x) \approx \bar{u}_s(x) \approx d_s(x) \approx \bar{d}_s(x) \approx s_s(x) \approx \bar{s}_s(x) \equiv S(x)$ ). When studying the small momentum part of the proton (i.e. at  $x \approx 0$ ) one probes the low momentum sea quarks. On the other side of the spectrum, at high momenta (i.e. at  $x \approx 1$ ), the high momentum valence quarks leave little unoccupied room for the sea quarks and thus one probes the valence quarks mainly. This is experimentally illustrated in fig. 1.13, where obviously depending on the value of  $x$  one can probe either the valence and sea quarks (i.e. at high values of  $x$ ) or the sea quarks (i.e. at low values of  $x$ ).

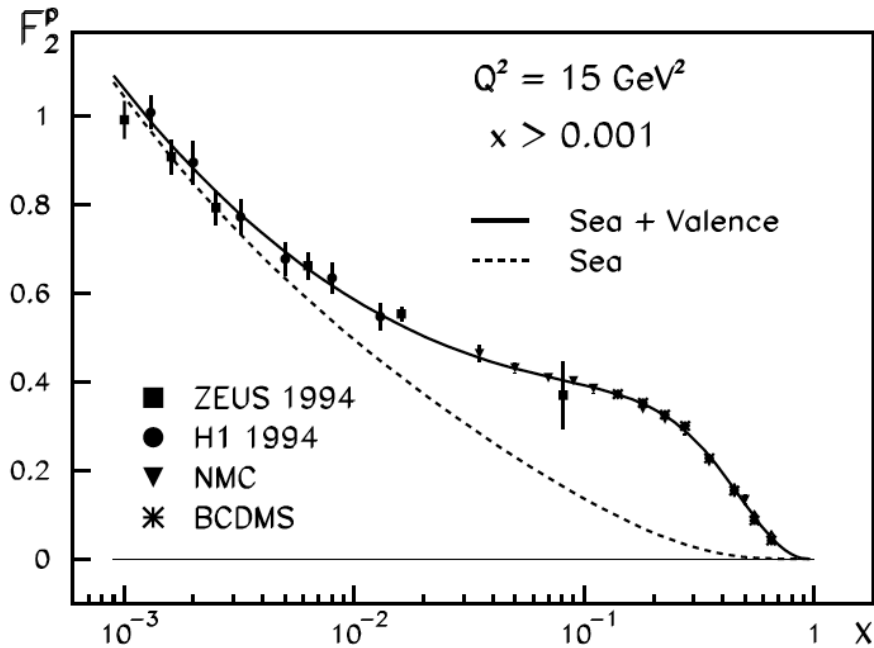


Fig. 1.13: The proton structure function as measured experimentally as a function of Bjorken- $x$ . At different values of  $x$  one probes either the sea or the valence and sea quarks.

Finally integrating the quark distributions obtained from deep inelastic charged lepton and neutrino scattering gives

$$\sum_i \int_0^1 x f_i(x) dx \approx 0.5$$

The missing momentum turns out that is carried by gluons. Introducing a gluon momentum distribution  $xg(x)$ , the correct momentum sum rule is

$$\sum_i \int_0^1 x f_i(x) dx + \int_0^1 xg(x) dx = 1$$